Magnetic phenomena, spin-orbit effects, and Landauer conductance in Pt nanowire contacts: Density-functional theory calculations

Alexander Smogunov,[1,2,3] Andrea Dal Corso,[2,4] and Erio Tosatti[1,2,4]

[1]*International Centre for Theoretical Physics (ICTP), Strada Costiera 11, I-34014 Trieste, Italy*
[2]*INFM Democritos National Simulation Center, Via Beirut 2-4, I-34014 Trieste, Italy*
[3]*Voronezh State University, University Square 1, Voronezh, Russia*
[4]*International School for Advanced Studies (SISSA), Via Beirut 2-4, I-34014 Trieste, Italy*

Platinum monatomic nanowires were predicted to spontaneously develop magnetism, involving a sizable orbital moment via spin-orbit coupling, and a colossal magnetic anisotropy. We present here a fully-relativistic (spin-orbit coupling included) pseudopotential density functional calculation of electronic and magnetic properties, and of Landauer ballistic conductance of Pt model nanocontacts consisting of short nanowire segments suspended between Pt leads or tips, represented by bulk planes. Even if short, and despite the nonmagnetic Pt leads, the nanocontact is found to be locally magnetic with magnetization strictly parallel to its axis. Especially under strain, the energy barrier to flip the overall spin direction is predicted to be tens of meV high, and thus the corresponding blocking temperatures large, suggesting the validity of static Landauer ballistic electrical conductance calculations. We carry out such calculations to find that inclusion of spin-orbit coupling and of magnetism lowers the ballistic conductance by about $15 \div 20\%$ relative to the nonmagnetic case, yielding $G \sim 2G_0$ ($G_0 = 2e^2/h$), in good agreement with break junction results. The spin filtering properties of this highly unusual spontaneously magnetic nanocontact are also analyzed.

I. INTRODUCTION

Metallic nanocontacts as thin as one atom can be fabricated, imaged, and studied by means of several experimental techniques including tip based instruments, transmission electron microscopy, and mechanically controllable break junctions. In the latter, metal nanocontacts often break at the stage of single-atom contact; in addition in some cases, short one-dimensional chains of atoms can be obtained prior to breaking.[1,2] It was shown experimentally[3] and theoretically[4,5] that the formation of such atomic chains (monatomic wires) is favored in heavy $5d$ metals such as Ir, Pt, and Au. In Au, short suspended monatomic wire segments were first imaged experimentally by transmission electron microscopy[1,6,7] and their conductance, close to unity, characterized in break junctions.[8] Pt monatomic suspended nanowires were also characterized with similar methods.[3,9]

Due to the nanometric dimensions, electron transport in atomic-sized nanocontacts is essentially ballistic. For a nonmagnetic contact, or for a statically magnetized one, ballistic conductance is given in the linear response limit by the Landauer-Büttiker transmittance, $G = (1/2)G_0 \Sigma_i T_i(E_F)$, where $G_0 = 2e^2/h$ is the conductance quantum and $T_i(E_F)$ is the transmission probability at the Fermi energy for the conductance channel i. In a nanocontact with a single atom cross section the number of conductance channels is controlled by the atom valency. The simplest case of monovalent metals such as Au, Ag, and Cu presents just two s-like channels (one per spin) with almost perfect transmission so that the conductance is close to G_0. In transition metals with partially occupied d orbitals (e.g., Pt, Pd, Ni, Co, etc.) in addition to two s channels there are several d channels also contributing to electron transport. This leads to a rather broad first peak centered well above G_0 in the conductance histograms. Here

we shall be concerned with the case of Pt, of special interest owing to its proximity to magnetism, and to its known ability to form nanowires.[3]

In Pt, a variety of values for the position of the first conductance peak has been reported ranging from 0.5 G_0 to 2.5 G_0.[3,9–16] The origin of the subpeaks at 0.5 G_0 and 1 G_0 was later attributed to the presence of gas molecules[15–18] possibly forming bridges between the electrodes just before contact breaking. For clean Pt nanocontacts data generally show a broad conductance histogram first peak centered between 1.5 G_0 and 2 G_0.[3,12–16] To date there has been a variety of theoretical studies on electron transport in Pt nanocontacts.[17–22] Recent calculations[18,19] based on density functional theory and on the Landauer-Büttiker formulation reported conductances close to 2 G_0 for single-atom contacts and for straight monatomic wires and lower values (down to 1.5 G_0) for zigzag nanowires.

However, approaches used so far were mostly restricted to the scalar-relativistic level where spin-orbit coupling (SOC) is absent. Furthermore, only in one case magnetic effects have been considered in the calculation of the ballistic conductance.[21] Actually, Pt is a Stoner enhanced, nonmagnetic material in bulk; however, the tendency toward magnetism is expected to get stronger in monatomic chains[23] for two reasons. The first is that the narrowing of d bands caused by the lower atomic coordination acts to enhance the electronic density of states (DOS) at the Fermi energy to approach and eventually to exceed the Stoner instability limit. This effect is especially pronounced in one-dimensional Pt monatomic wires where van Hove band-edge singularities fall near the Fermi level.[23,24] The second reason stems from SOC, which reinforces spin magnetism with an accompanying orbital moment. In a Pt monatomic wire, SOC acts to stabilize magnetism, raising a sizeable parallel orbital mo-

ment to accompany a nonzero spin moment, even at the equilibrium interatomic distance. In density functional calculations, a spin-orbit split electronic band edge is pushed up closer to the Fermi level driving the infinite monatomic nanowire to a ferromagnetic ground state.[23,24]

Our interest here is on the conductance of a monatomic Pt nanocontact, on the role of SOC, and on the effect of local magnetization if present. Because magnetization in a ("zero-dimensional") nanocontact will generally fluctuate, a static calculation such as that given here, and the use of the Landauer-Büttiker approximation to the conductance are not in principle adequate. Very close to zero voltage, dynamical phenomena such as Kondo anomalies may affect the conductance. In the present study we will leave this regime aside and defer these interesting dynamical phenomena to a later study. We will therefore focus on the basic Landauer-Büttiker static level. This should be adequate at small but finite voltages above possible zero-bias anomalies. Our calculations will demonstrate chiefly the role of SOC and of local magnetism on the nanocontact ballistic conductance. They will also demonstrate that the recently discussed property of colossal magnetic anisotropy and of large energy barriers against flip of magnetization[24] should also apply to monatomic nanocontacts, with the interesting consequences of large "blocking" temperatures.

We recently presented an approach suitable for calculating the Landauer-Büttiker conductance based on a generalization of the method of Choi and Ihm[25] to the case of fully-relativistic (FR) ultrasoft pseudopotentials (USPPs).[26] In Ref. 27 we showed that these PPs can reproduce accurate electronic band structures of fcc-Pt and fcc-Au calculated by solving a four-component Dirac equation, within a scheme based on two-component spinors. In this paper, we will use these FR USPPs to study theoretically short monatomic Pt wires suspended between two bulk Pt leads and address several important issues. First, does the suspended nanowire segment remain locally magnetic even when just a few atoms long, and despite being attached to bulk nonmagnetic leads? Also, since we will find that this is the case, what is the role of the wire's length and strain on the local nanowire magnetism? Furthermore, in the presence of SOC, does the nanowire contact still exhibit giant or colossal magnetic anisotropy and the large energy barrier to magnetization reversal characteristic of the infinite nanowire? What is the joint effect of SOC and of magnetism on the ballistic conductance of Pt model nanowire contacts? And finally, how spin selective will the conductance be, and what kind of spin filtering would the static local magnetization exert on the current? The answer to these questions, so far unknown, should provide new basic information on the physics of these unconventional nanocontacts, with an underlying potential and interesting connection between magnetism and conductance.

II. INFINITE MONATOMIC WIRE

Before focusing on Pt nanowire contacts we will begin by presenting some results for the idealized case of an infinite tipless monatomic wire, which reproduce those recently published by us and by others.[19,21,24] Electronic structure calculations were carried out within the density functional theory, using the standard plane-wave PWscf code of the Quantum-ESPRESSO package.[28] The local-spin-density approximation (LSDA) in the form introduced by Perdew-Zunger[29] is used for the exchange-correlation energy.[30] We performed both scalar-relativistic (SR) and FR pseudopotential calculations. In the first case, the Pt ions are described by USPPs generated with all relativistic corrections except of the spin-orbit coupling. In the second case, the fully-relativistic USPPs (with spin-orbit included) are used to simulate Pt ions and electron wave functions are two-component spinors. The parameters of the PPs are given in Ref. 27. The cut-off kinetic energies were 30 Ry and 300 Ry for the wave functions and for the charge density, respectively. Integration over the Brillouin zone (BZ) up to the Fermi energy was performed by using 320 one-dimensional k points with a smearing parameter of 0.002 Ry.[31]

Both SR and FR total energy minimizations for an infinite Pt wire yield a zero strain nanowire equilibrium interatomic distance $d_0 \approx 2.35$ Å. However, while the SR calculation predicts the unstrained Pt wire to be nonmagnetic, the FR calculation yields for the same system a ferromagnetic ground state with the magnetization parallel to the wire, in agreement with earlier calculations of Delin *et al.*[23] The calculated spin and orbital moments per atom at d_0 are $M_{S\parallel}$ =0.17 μ_B and $M_{L\parallel}$=0.22 μ_B, respectively. Furthermore, the magnetization magnitude vanishes if its direction is constrained to lie perpendicular to the wire. A magnetic state with transverse magnetization actually becomes stable with strain, but only at much larger interatomic distances (above 2.6 Å), and even then at a much higher energy than the nanowire ground state with parallel magnetization. Thus the equilibrium and low strain Pt nanowire displays a *colossal* magnetic anisotropy with the easy axis parallel to the wire.[24] The (zero-temperature) infinite Pt nanowire is actually quite a strong magnet, especially when strained. We gauged for example the strength of interatomic magnetic exchange by forcing a magnetization reversal and found an energy increase of about 85 meV at d=2.66 Å. In a localized picture of magnetism, this would be equivalent to a near neighbor intersite exchange magnitude of nearly 500 K.

Interatomic distances at break junction nanocontacts are generally under heavy strain. Measured break junction forces in fact generally lie above 1 nN.[32] Especially at criogenic conditions where atomic mobility is largely frozen out, stress and strain are generally speaking not well characterized. At larger temperatures, and in conditions of quasiequilibrium, it can be argued that a finite spontaneous stress tension should be present even when the tips are kept at fixed distance without any pulling force.[5,33] In our nanowire study we arbitrarily choose strains ranging from an interatomic Pt-Pt distance d =d_0=2.35 Å (zero strain) to d=2.66 Å which corresponds to a strained nanowire, with a tension of approximately 3.8 nN, roughly in the range of spontaneous breaking (we checked that a nanocontact formed by a three-atom segment of such a strained nanowire is still stable; see Sec. III). At this interatomic distance the infinite wire is still nonmagnetic within the SR scheme, where SOC is absent, whereas in the more correct FR case which includes SOC, the wire is strongly ferromagnetic. The colossal magnetic anisotropy
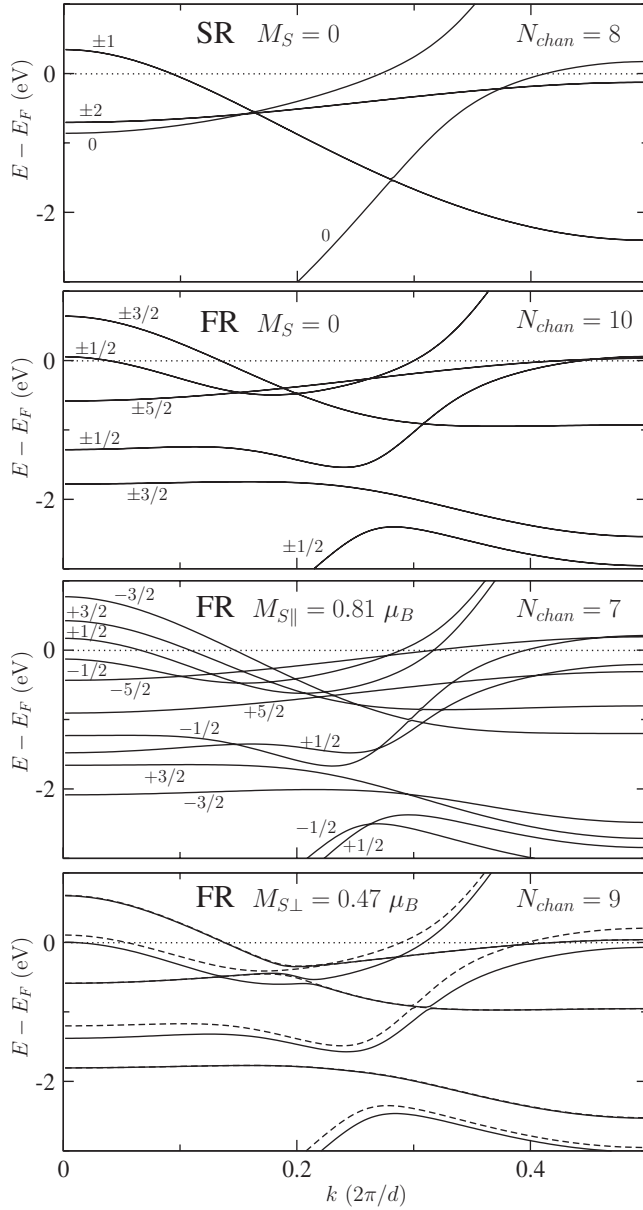
FIG. 1. Electron band structure of the infinite monatomic Pt wire with interatomic distance of 2.66 Å calculated with SR (upper panel) and FR (lower panels) pseudopotentials. For the FR, more realistic case, the bands for nonmagnetic as well as for both magnetic polarizations (magnetic moment parallel or perpendicular to the wire axis) are shown. The bands are labeled according to their symmetry (see text). The number of bands crossing the Fermi level (number of conductance channels) is provided on each panel. The spin magnetic moment per atom is also given for magnetic states.

here reverts to a conventional giant anisotropy[34–36] with an easy magnetization axis parallel to the wire and an extremely large anisotropy energy, $E_\perp - E_\parallel \approx 36$ meV/atom.

Qualitatively relevant to our subsequent reasoning on electron transport is the number of conductance channels N_{chan}, that is the number of bands crossing the Fermi level. In Fig. 1 we show the electron band structure of the infinite Pt monatomic nanowire calculated in the SR and FR schemes. In the latter case SOC splits the bands in the (artificially forced) nonmagnetic state, and magnetism further splits them

corresponding to majority and minority polarizations. The ballistic conductance channels are clearly seen to change from one case to another.

Although unrealistic in practice, the infinite nanowire is important because it lends itself to understand symmetry aspects. We classify the electronic bands as follows: In the SR case the Hamiltonian commutes with $\hat{L}_z$, the projection of the orbital angular momentum on the wire axis (the z axis) so that electron states can be labeled by its eigenvalues $m = 0, \pm 1, \pm 2$, etc. (in units of $\hbar$). Bands with $\pm m$ are degenerate due to the mirror symmetry with respect to a plane such as xy containing the wire axis. This classification corresponds to one-dimensional ($m = 0$) and two-dimensional ($m = \pm 1, \pm 2$, etc.) irreducible representations of the symmetry group $C_{\infty v}$. Moreover, all bands possess additional degeneracy due to spin, since the spin and orbital degrees of freedom do not mix in the SR case. In the FR case, the spin and orbital degrees of freedom are coupled through SOC and the bands are now labeled by half-integer eigenvalues $m_j = \pm 1/2, \pm 3/2, \pm 5/2$, etc. of the operator $\hat{J}_z$, the z-component of the total angular momentum. In the nonmagnetic state, again due to the mirror symmetry in the xy plane (and also due to time-reversal symmetry in conjunction with inversion symmetry) the bands with $\pm m_j$ (an infinite number of two-dimensional irreducible representations of the double group of $C_{\infty v}$) are degenerate. The twofold degeneracy of these nonmagnetic states is lifted when the wire is magnetized in the parallel direction since reflection (as well as time reversal) is no longer a symmetry operation. Magnetization, an axial vector, reverses its direction under both spatial reflection in the xy plane and under time reversal, but not under inversion. This lifting of degeneracy corresponds to a reduction of the symmetry group from $C_{\infty v}$ to C_∞, the latter with one-dimensional irreducible representations only. In the state with transverse magnetization (lower panel), the only remaining symmetry is a reflection through the plane containing the wire axis and perpendicular to the magnetization. The symmetry double group is C_s^D with two one-dimensional irreducible representations Γ_3 and Γ_4. Hence, all bands separate here into two groups transforming according to Γ_3 or Γ_4 shown by solid and dashed lines, respectively.

We find that the number of conductance channels is modified both by spin-orbit interactions and by magnetism. Comparing the two upper panels we see for example that the spin-orbit interaction splits four $m = \pm 2$ bands into the pair of twofold degenerate bands with $m_j = \pm 3/2$ and $m_j = \pm 5/2$. With SOC, but still no magnetism, the bands with $m_j = \pm 5/2$ are pushed up in energy to now cross the Fermi level so that the number of conductance channels is increased from eight to ten. We note that there are three twofold degenerate bands (one with $m_j = \pm 5/2$ and two with $m_j = \pm 1/2$) with edges very close to the Fermi energy, which results in an exceedingly large DOS at the E_F. Upon onset of parallel ferromagnetism, this band edge near E_F is split by magnetic exchange, one majority band now completely full, and a minority band further emptied. Nanowire magnetization lowers the DOS at E_F, corresponding to a sort of band Jahn-Teller effect.[24] With parallel magnetization three conductance channels altogether drop out compared to the non-

magnetic state, whence now $N_{chan}=7$. The number of conductance channels increases by two, from seven to nine, when the magnetization is rotated from parallel to perpendicular to the wire axis. The corresponding change in conductance with the magnetization direction, also termed "anisotropic magnetoresistance (AMR)" can be characterized by the ratio $(G_\perp - G_\parallel)/G_\parallel$. Our infinite nanowire calculations thus foreshadow a large AMR even in real Pt contacts, provided they will develop a spontaneous magnetic moment, and provided that the moment could be rotated with practically attainable external magnetic fields. We will see later that while the former is confirmed, the required field to rotate magnetization in a Pt contact may generally be very large and hard to reach in practice. In the present academic case of the infinite nanowire, AMR $=(N_{chan,\perp}-N_{chan,\parallel})/N_{chan,\parallel} \approx 28\%$.

III. MONATOMIC NANOWIRE CONTACT: MAGNETIC PROPERTIES

After the academic infinite nanowire, we considered model Pt contacts, made up of a short N-atom linear chain segment suspended in vacuum between two semi-infinite ideal Pt bulks. In line with real break junction data,[3] we considered contacts with $N=3$, 4, and 5 atoms in the chain. The contacts consist of the supercell depicted for $N=3$ in the inset of Fig. 2. The nanowire segment is attached at "hollow" sites of two mirror symmetrical Pt(001) surfaces. For calculations, a $(2\sqrt{2} \times 2\sqrt{2})$ supercell periodicity is employed in the xy plane, perpendicular to the nanowire. We checked that this spacing is enough to keep the periodically repeated wires sufficiently apart from one another to make their mutual influence irrelevant. The bulk "leads" are simulated by a planar slab consisting of seven atomic (001) crystalline planes (eight atoms per plane), sufficient to reproduce a bulk-like potential in the middle of the slab. Periodic boundary conditions are assumed in all three directions for electronic structure calculations. Since the supercell is very large along [001] (the z axis), the BZ in this direction is sampled only at $k_z=0$ while in the (k_x,k_y) plane perpendicular to the wire convergence demanded instead ten two-dimensional (2D) special **k** points. This level of BZ sampling was checked for accuracy and found to be sufficient for obtaining a converged self-consistent potential needed for subsequent transmission calculations. The energy smearing parameter near E_F was chosen to be 0.01 Ry.

Atoms of the seven-layer slab representing the bulk leads are located at their ideal bulk fcc positions (with interatomic spacing of 2.77 Å). The interatomic distance in the nanowire for all the contacts was kept at the same strained value earlier chosen for the infinite nanowire, namely $d=2.66$ Å. The distance between the (001) surface planes and the last contact nanowire atoms was 1.91 Å, a value obtained by prior SR calculations of the three-atom contact and optimization moving the contact nanowire atoms until forces acting on them vanished (we note that in doing so we were also changing the length of the supercell in the z direction). We checked that this geometry corresponds to a strained but still unbroken chain nanocontact.

The main result is that for all chain lengths N the Pt nanocontacts develop local magnetism. In Fig. 2 we plot the pla-
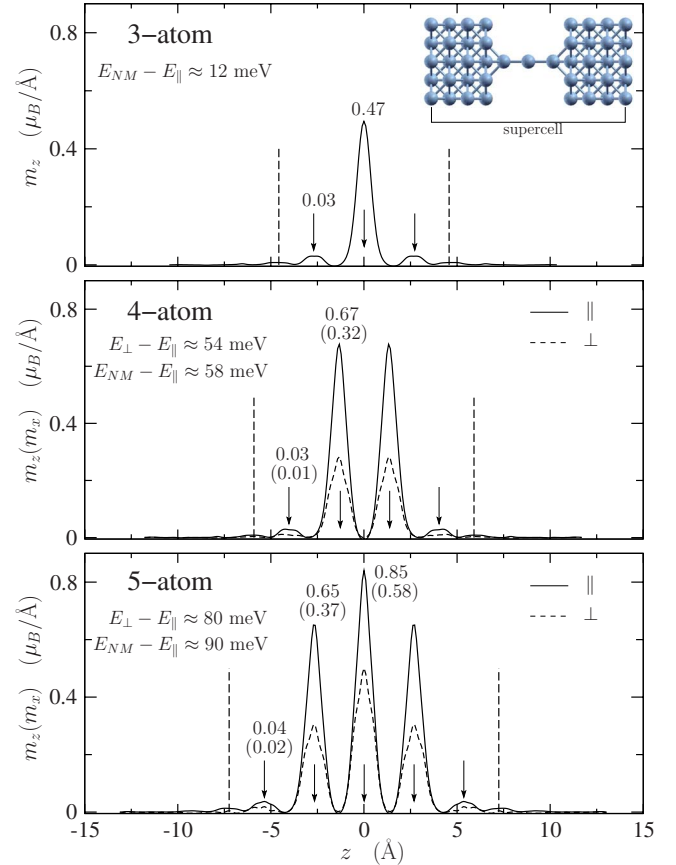

FIG. 2. (Color online) Planar average (in the xy plane) of the spin magnetization as a function of z for three-, four-, and five-atom Pt nanowire contacts calculated with FR pseudopotentials. The magnetic states with parallel and perpendicular polarization in the four- and five-atom case are shown by solid and dashed lines, respectively. The magnetic moments (in Bohr magnetons) within a sphere with radius of 2.5 Å are shown for all nanowire atoms. The vertical dashed lines show the positions of the bulk lead surfaces; the positions of nanowire atoms, with a mutual spacing of $d=2.66$ Å, are indicated by arrows.

nar average (in the xy plane) of the spin magnetization as a function of z for the nanowire contacts of different lengths calculated with FR pseudopotentials, fully including SOC. We discuss first the three-atom nanocontact (upper panel). Starting with the three chain atoms magnetized in the parallel direction (as in the ground state of the infinite wire) we found that the nanocontact remains locally magnetic despite being in strong contact with nonmagnetic bulk Pt leads. The local magnetization is maximum at the central nanowire atom and is significantly suppressed at the contact atoms touching the nonmagnetic Pt leads. The central nanowire Pt atom has a spin moment of 0.47 μ_B, to be compared with the corresponding value for the infinite wire (0.81 μ_B). The *total* nanocontact spin magnetic moment $M_{S\parallel}^{tot}$ was 0.56 μ_B. Of this, about 0.03 μ_B is due to evanescent magnetization tails propagated from the magnetic Pt chain into the two bulk leads. Starting next with an initial magnetization transverse to the chain, we found that at $N=3$ this polarization does not survive, converging to a nonmagnetic nanocontact state. The infinite nanowire transverse magnetization, already weak

from the beginning, is in this case suppressed by the non-magnetic bulk Pt leads so that such contact displays the property of colossal magnetic anisotropy.[24]

The influence of the nonmagnetic leads is expected to weaken for increasing nanocontact chain length N. The results for $N=4$ and 5 are shown in Fig. 2 on two lower panels. In these longer nanocontacts both magnetic states with parallel and transverse magnetizations are sustained. The corresponding magnetization curves are shown by solid and dashed lines for the parallel and transverse case, respectively, showing that magnetism indeed becomes more robust with increasing nanocontact chain length. For example, in the ground state (magnetization parallel to the wire) the magnetic moment of the chain central atom grows from 0.47 μ_B ($N=3$) to 0.67 μ_B ($N=4$), and further to 0.85 μ_B ($N=5$). The latter is in fact slightly larger than the magnetic moment per atom in the infinite wire (0.81 μ_B), a slight overshoot possibly related to surface induced interference effects. The total nanocontact spin magnetic moment here was $M_{S\parallel}^{\text{tot}}$ $=1.44$ μ_B and $M_{S\parallel}^{\text{tot}}=2.29$ μ_B for four- and five-atom nano-contacts, respectively. The amount of spin moment spread in the bulk leads is therefore about 0.04 μ_B ($N=4$) and 0.06 μ_B ($N=5$), still a very small fraction of the total moment. The Pt atoms in the nanowire clearly drive the magnetization, but at least in this geometry a giant moment[37] apparently does not form.

We also obtained the total energies Δ of various metastable states above the parallel magnetic ground state. The transversely magnetized state has a much higher energy than the ground state, about $\Delta_\perp=50$ meV and $\Delta_\perp=80$ meV for the four-atom and five-atom wires, respectively. The three-atom contact does not have a transversely magnetized state, but there is still a barrier of $\Delta_{\text{NM}}=12$ meV between the two equivalent parallel magnetization ground states. We did not repeat the nanocontact calculations for general chain interatomic distances d. The qualitative result can still be roughly estimated by simply rescaling infinite wire ground state energies of Ref. 24 and assuming a total of $N-2$ equivalent magnetic Pt atoms in the nanocontact. In that way we anticipate that for example at $d=2.5$ Å, for all $N=3-5$ there should be a (parallel) magnetized ground state but no transversely magnetized state whatsoever (colossal anisotropy) with an estimated barrier between the two parallel polarizations about 10–30 meV. These large magnetic anisotropy barriers should effectively impede the rotation and/or the flip of the nanocontact magnetization as a whole. A high barrier should also to some extent hamper fluctuations. While a detailed appraisal and treatment of fluctuation effects is beyond the scope of this work, we can still use this result for some tentative conclusions. As a consequence of the high barrier, a full magnetization reversal due to occasional transverse anisotropies and/or thermal fluctuations should be rare. Local spin fluctuations that renormalize but do not reverse magnetization become competitive with the global ones. Interestingly, the Zeeman coupling energy $\mu_B B M_S^{\text{tot}}$ of an external field B may only match the magnitude of the anisotropy barrier at field values as large as 100 Tesla. Therefore, the anticipated effect of a field of ordinary magnitude is negligible.

We tentatively conclude that the Pt nanowire contact is in effect an Ising-type nanomagnet with a large blocking temperature ($k_B T \sim 10$–50 meV), and thus with utterly infrequent thermal magnetization flips at criogenic temperatures. This assessment will need a revision at reduced or zero strains, where the chain interatomic distances may approach their minimum value near $d_0=2.35$ Å and nanowire magnetism, though still finite, becomes weaker. The nanocontact in this regime should still exhibit the property of colossal anisotropy the possible consequences of which will be examined elsewhere.

IV. BALLISTIC CONDUCTANCE

The main measurable physical quantity in a nanocontact is its electrical conductance. We calculated the ballistic electron conductance within the Landauer-Büttiker linear response formalism, appropriate as was discussed above when all the system parameters, including magnetization, can be treated as static. At sufficiently small voltage, ballistic conductance G is proportional to the total electron transmission at the Fermi energy, $G=(1/2)G_0 T(E_F)$. In order to calculate the nanocontact transmission we considered the geometry shown in Fig. 2 as the nanocontact scattering region, to be joined ideally to semi-infinite bulk Pt leads on both sides. The scattering problem between incoming and outgoing Bloch waves is then solved using the complex band method (for details see Refs. 25 and 38), whereby the transmission matrix and the total transmission is subsequently computed. For our plane-wave based FR calculations we use a recent extension of a method[26] accounting for SOC effects, and including proper treatment of two-component spinor Bloch wave functions. Since the system has the supercell (artificial) 2D periodicity in the xy plane, perpendicular to the transport direction, we averaged the transmission over the corresponding 2D BZ using 21 **k** points in the irreducible part of the BZ. This level of sampling was found to be needed and sufficient to get rid of spurious oscillations in transmission function and yields our best approximation to electron transmission in the true isolated nanocontact.

We started with the SR calculation for the three-atom nanowire contact and present in Fig. 3 the transmission function (per spin) versus the energy. In this approximation the Pt nanocontact is nonmagnetic. In order to understand the various features in the transmission curve we plot on the lower panels the local density of states (LDOS) projected on different atomic orbitals of the middle nanowire atom. At energies $E-E_F>0.5$ eV the transmission is very close to 1. In this energy region in the infinite wire there is only one s-p_z-like band for each spin (see upper panel of Fig. 1). This is a very broad band, with high kinetic energy states which generally exhibit very little reflection by obstacles such as the nanocontact, yielding nearly free propagation and transmission close to unity. At lower energies the d states make their appearance and the transmission starts growing significantly. The main contribution here comes from d_{xz}, d_{yz} states which form quite broad $m=\pm 1$ bands in the infinite wire. Just below the Fermi energy one can see several sharp features in the LDOS both for $s, d_{3z^2-r^2}$ and for $d_{xy}, d_{x^2-y^2}$ orbitals which are related to narrow nanowire bands of $m=0$ and of $m=\pm 2$ symmetry, respectively, lying close to the Fermi
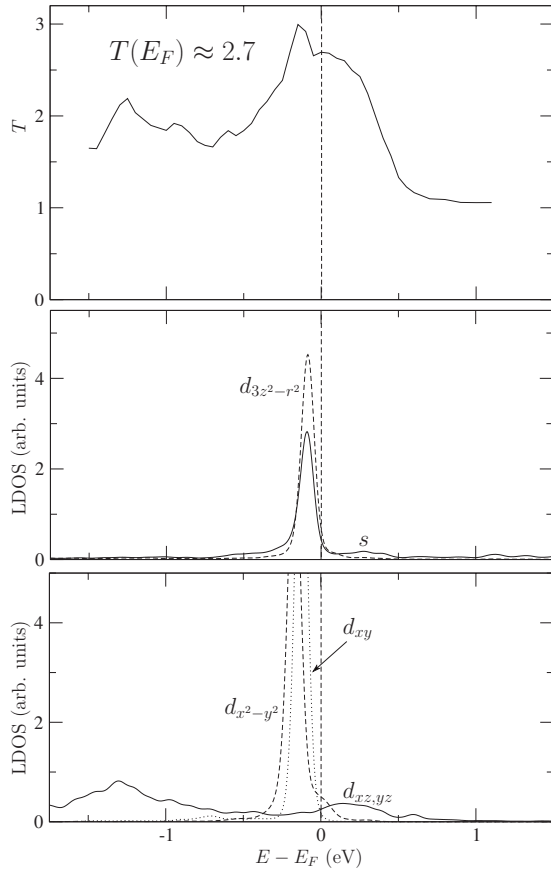
FIG. 3. Transmission coefficient (per spin) versus energy for the three-atom nanowire Pt contact at $d=2.66$ Å (upper panel) in the SR approximation, where spin-orbit coupling is not included, and the contact is nonmagnetic. Note the anticipated value of ballistic conductance of 2.7 G_0, considerably higher than typical experimental values in the range 1.5–2.0 G_0. The lower panels show the LDOS projected on different atomic orbitals of the middle nanowire atom.

energy. These LDOS peaks give rise to the sharp feature in the transmission function at the energy $E-E_F \sim -0.2$ eV. From the transmission at the Fermi energy we obtain the ballistic conductance of about 2.7 G_0. The transmission curve shown in Fig. 3 looks quite similar to that presented recently by Fernández-Rossier *et al.*[21] who, with a slightly different geometry and larger interatomic distances in the nanowire, found the conductance of about 2.3 G_0. Our conductance is also somewhat higher than the values of ~ 2 G_0 calculated for straight monatomic Pt wires in Refs. [18] and [19]. Break junction experiments generally report a broad peak in conductance histogram centered at values between 1.5 G_0 and 2 G_0.[3,12–16] Recently, Nielsen and coworkers[14] argued that even lower conductances (down to 1.5 G_0) should be assigned to monatomic wires while single-atom contacts should have conductances close to 2 G_0.

We now turn to FR ballistic conductance calculations, our best approximation. We collect and compare in Fig. 4 the SR and FR results for nanowire contacts of different lengths N =3, 4, 5. On the right side of the figure we also mark the nominal maximum "conductances" for the ideal infinite monatomic wire for each case, $G=(N_{chan}/2)G_0$ (see Fig. 1).
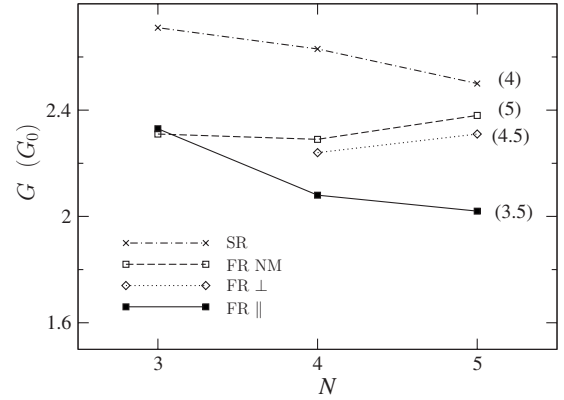

FIG. 4. Ballistic conductance of three-, four-, and five-atom nanowire Pt contacts. Here SR and FR calculations are compared including in the latter case, the conductances for both parallel and transverse magnetic states as well as for the nonmagnetic state. The FR state with parallel magnetization corresponds to the nanocontact ground state, with a ballistic conductance of about 2 G_0. The ideal contactless maximal conductance of a perfect infinite nanowire (deduced from the channel number in the band structure of Fig. 1) is also provided for each case.

As a general effect, we see that the conductance is lowered when SOC is included. For the three-atom nanocontact the FR conductance is about 2.3 G_0 for both magnetic and nonmagnetic states, about 15% lower than the SR conductance (~ 2.7 G_0). This result could not have been anticipated from a simple consideration of the infinite nanowire bands of Fig. 1—one could rather have expected the highest conductance for the FR nonmagnetic state ($N_{chan}=10$) relative to the SR case ($N_{chan}=8$), and finally a much lower conductance for the magnetic state ($N_{chan}=7$). Such differences originate mainly from the shortness of the nanocontact—a three-atom nanowire is far from infinite. Magnetism is significantly weakened (see upper panel of Fig. 2), and, as a consequence, so are the effects of magnetism on conductance.

When the nanowire becomes longer the magnetism in the nanowire gets stronger. Conductance through the magnetic nanocontact drops down to ~ 2 G_0 and differs more and more from that of the nonmagnetic state. For $N=5$ this difference is as large as 0.4 G_0. We note that recently Fernández-Rossier and coworkers[21] performed SR calculations (where spin-orbit effects were disregarded) and also reported the formation of magnetic moment in Pt nanowires under some significant strain. They also found that the conductance is lower for the magnetic state, in agreement with our calculations.

For nanocontacts with $N=4$ and 5, we calculate and predict anisotropic magnetoresistance, namely the state with transverse magnetization has a higher conductance than the (ground) state with parallel magnetization. Our calculations predict an AMR of ~ 8% and ~ 15% for $N=4$ and 5, respectively. Note that these values for AMR are still noticeably smaller than the ideal value given earlier for an infinite nanowire (~ 28%). We underline again, however, that due to the high barrier it should be generally very hard if not impossible to turn the magnetization away from the parallel direction, and measure directly the AMR of a Pt nanocontact with practically attainable fields.

Looking at conductances of various states of the five-atom Pt nanocontact one can see that, unlike the case of a shorter three-atom wire, they are now arranged almost in the same order as those of the ideal infinite wire. The only remaining disagreement is for the SR conductance—it is still higher than the conductance of, e.g., FR nonmagnetic state. This can be rationalized by looking at the bands of Fig. 1 and noticing that even though the number of conductance channels is larger for the FR nonmagnetic state than for the SR case (ten against eight) some of the bands touch the Fermi level close to their very edges. Here the electron group velocity is small, and so is the contribution to conductance.

V. DISCUSSION AND SPIN FILTERING PROPERTIES

The above density functional calculations show that short but well-defined monatomic nanowire segments forming at Pt nanocontacts should be spontaneously magnetic. The overall magnetic energy gain increases with the number of atoms in the wire and with the strain. It is quite large, reaching up to 90 meV for $N=5$ and large strains. For the chosen nanowire interatomic distance $d=2.66$ Å, the magnetic anisotropy is also exceedingly large—"colossal" for $N=3$ and "giant" for $N=4$, 5, the easy magnetization axis parallel to the nanowire. Ballistic conductance is sensitive to the onset of local magnetism, whose presence causes a drop of the order of 10% relative to the nonmagnetic state (a state which however is unstable).

The question is, whether and how it will be possible to obtain a direct experimental evidence of the presence of nanocontact magnetism in Pt, a task which is not easy at the present stage. The most common type of evidence of magnetism at quantum dot and molecular nanocontacts is a Kondo zero-bias anomaly.[39] We note here that our system is not a regular Kondo system, on account of giant anisotropies and of other elements including proximity to ferromagnetism in the leads, and will defer this aspect for the time being, and concentrate on bias voltages slightly away from zero, where these effects should be irrelevant. Here, assuming the time of traversal of a ballistic electron is short enough, the nanocontact should effectively exhibit a static or slowly varying magnetic moment, with some interesting even if speculative consequences.

One of them is a spin filtering effect. In ferromagnetic nanocontacts (such as Ni or Co) majority and minority spin channels have very different conductances, the former smaller than the latter, which leads to a spin-polarized current in the steady state. The effect of that may be difficult to detect on account of the large preexisting spin polarization of the leads. In Pt nanocontacts, the advantage is that the leads are not magnetic, and therefore any evidence of magnetism can be safely attributed to the nanocontact. In order to illustrate the possibility of a spin-polarized net current for our *locally* magnetized Pt nanocontacts, we show in Fig. 5 the eigenchannel decomposition of the total FR transmission at the Fermi energy as a function of N calculated at the $\bar{M}$ point of the 2D BZ. We label all the eigenchannels by half-integer m_j as follows: Since the nanocontact chain is magnetic in parallel direction, the symmetry group of the $\bar{M}$ point (and
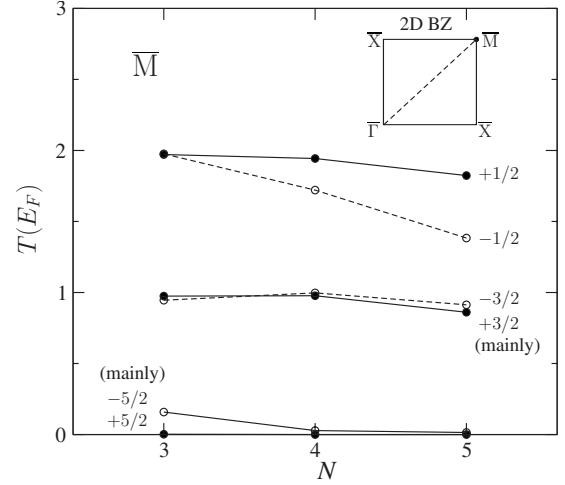

FIG. 5. Eigenchannel decomposition of the FR total transmission at the Fermi energy calculated at the $\bar{M}$ 2D **k** point (see the inset). Here (as well as at the $\bar{\Gamma}$ point), due to the symmetry, the half-integer m_j can be assigned to each transmission eigenchannel (see text).

also of the $\bar{\Gamma}$ point) is the double group of C_4, the group of our slab. All transmission eigenchannels can be classified according to its four one-dimensional irreducible representations, in turn expressible as linear combinations of representations of the larger infinite nanowire group C_∞, labeled by all half-integer m_j. In this way, m_j and m_j+4n (with n integer) can mix to form the same representation of C_4 double group and the corresponding states will generally get mixed in the presence of square symmetry contacts. This is the case, for example, for $+3/2$ and $-5/2$ as well as for $-3/2$ and $+5/2$ states.

We note that, as illustrated in Fig. 5 for the $\bar{M}$ **k** point, magnetism causes in general a conductance imbalance between $+m_j$ and $-m_j$ channels (here, mainly between $\pm 1/2$ channels) which becomes larger for longer wires due to stronger magnetism. Therefore, as current flows through the Pt nanocontact, there will be an accompanying magnetization (spin, and orbital) flow as well. During the time τ (presently unknown, but assumed long) while the nanomagnet magnetization direction does not flip, this should lead to a magnetization accumulation uphill, and a corresponding depletion downhill. The amount of accumulation is determined by the actual conductance filtering asymmetry, which we calculate by the current, which can be controlled, and by the rate of magnetization decay in the bulk Pt leads, which is uncontrolled but probably high on account of a large DOS at the Fermi level and large SOC. The actual calculated amount of selective filtering shown in Fig. 5 is not large, but even if modest, it could be important, because the Pt leads are themselves nonmagnetic, and all magnetic effects can only be attributed to the nanocontact itself. In fact, current in presence of local magnetism at the Pt nanocontact should alter the size and extent of the magnetization tails into the bulklike Pt leads. In particular, a ferromagnetic giant tail moment, absent in equilibrium, might be expected to form uphill of a nanocontact, previously prepared in a well-defined

polarization state by e.g., field cooling. In these conditions, a spontaneous reversal of magnetization would imply a large transient magnetic reorganization, the giant tail shifting from uphill to downhill. This could in turn reflect in an observable transient effect on conductance. However, the magnitude of this effect remains at this stage unpredictable.

VI. CONCLUSIONS

We carried out a fully-relativistic density functional study of electronic, magnetic, and transport properties of nanowire Pt contacts. We studied model nanowire contacts with $N=3$, 4, and 5 atoms in the wire and found that they remain locally magnetic despite the presence of nonmagnetic Pt leads, and that magnetism is stronger for longer wires and for larger strain. Spin-orbit effects are crucial to the phenomenon and give rise to a very large spin anisotropy for $N=4$ and 5 with easy axis along the nanowire. The energy of a transversely magnetized state is much higher, roughly ~ 50 meV and ~ 80 meV for $N=4$ and 5, respectively. For the shorter nanocontact with $N=3$ there is no transversely magnetized state, and the anisotropy is "colossal." These large barriers should provide a high blocking temperature below which thermal fluctuations are ineffective, and nanowire magnetism could be observed. Kondo phenomena are not addressed here, but are expected to be strongly influenced by anisotropy and by proximity to ferromagnetism in Pt.

From our calculated Landauer-Büttiker ballistic electron transport, we conclude that inclusion of both SOC and magnetism is important and lowers the ballistic conductance by about $15 \div 20\%$. The lowest conductance, $G \sim 2\ G_0$, occurs in the ground state with magnetization parallel to the wire. These values are close to those reported in break junction experiments ($G \sim 1.5$–$2.0\ G_0$). A conductance of 1.5 G_0 is however below our calculated value. During the breaking process, the symmetry of the nanocontact is expected in general to be lower than that implied by our assumed geometry. A lower symmetry might act to block some channels or anyway decrease their transmissions lowering even more the total conductance. For example, it has been recently shown that zigzag Pt nanowires have lower conductances ($\sim 1.5\ G_0$) with respect to the straight ones ($\sim 2\ G_0$). While we note that a zigzag configuration is expected to be removed by stress (which is the case in our study), this example does make the point. Moreover, the presence of

pyramid-like tips joining the nanowire to the bulk leads (disregarded in the present calculations) could also act to reduce the conductance. One can say, therefore, that our value of $G \sim 2\ G_0$ represents the higher estimate for the ballistic conductance in Pt nanowire contacts.

For long nanowire contacts ($N=4,5$) the conductance was found to increase when the magnetization is rotated and becomes perpendicular to the wire axis, a potential effect of AMR. We calculated the AMR magnitude of about 8% and 15% for $N=4$ and 5, respectively. The AMR could be in principle observed by applying a field to turn the magnetization perpendicular to the nanowire. However, due to the large magnetic anisotropy barrier the static deviation of the magnetization from the easy axis would be generally small for magnetic fields attainable in laboratory conditions. Quantum tunneling of magnetization,[40] although not discussed here and in principle not ruled out, should be strongly hindered by the large or colossal axial anisotropy, by temperature, and possibly by additional orthogonality phenomena due to the presence of the Fermi sea.

Our results suggest some qualitative hints for the possible observation of our predicted magnetic nanocontact phenomena, which at the moment remain exquisitely theoretical. It might still be possible to observe the effects of thermal or quantum flipping of magnetization in the form of noise in the current. Spin filtering effects could also be detectable. Other possibilities that emerged in discussions with experimentalists include conductance modifications at low voltage due to current induced dynamical changes of the magnetization profile, or detection of the moment by insertion of the Pt nanowire as a Josephson weak link between superconducting leads. Finally, Kondo zero-bias anomalies, although not addressed here, could provide a "smoking gun" for Pt nanowire magnetism.

[1] H. Ohnishi, Y. Kondo, and K. Takayanagi, Nature (London) **395**, 780 (1998).

[2] A. I. Yanson, G. Rubio Bollinger, H. E. van den Brom, N. Agrait, and J. M. van Ruitenbeek, Nature (London) **395**, 783 (1998).

[3] R. H. M. Smit, C. Untiedt, A. I. Yanson, and J. M. van Ruitenbeek, Phys. Rev. Lett. **87**, 266102 (2001).

[4] S. R. Bahn and K. W. Jacobsen, Phys. Rev. Lett. **87**, 266101 (2001).

[5] E. Tosatti, Solid State Commun. **135**, 610 (2005).

[6] V. Rodrigues and D. Ugarte, Phys. Rev. B **63**, 073405 (2001).

[7] T. Kizuka, Phys. Rev. B **77**, 155401 (2008), and references therein.

[8] N. Agrait, A. L. Yeyati, and J. M. van Ruitenbeek, Phys. Rep. **377**, 81 (2003).

[9] V. Rodrigues, J. Bettini, P. C. Silva, and D. Ugarte, Phys. Rev. Lett. **91**, 096801 (2003).

[10] L. Olesen, E. Laegsgaard, I. Stensgaard, F. Besenbacher, J. Schiøtz, P. Stoltze, K. W. Jacobsen, and J. K. Nørskov, Phys. Rev. Lett. **74**, 2147 (1995).

[11] J. L. Costa-Krämer, Phys. Rev. B **55**, R4875 (1997).

[12] J. M. Krans, C. J. Muller, I. K. Yanson, T. C. M. Govaert, R. Hesper, and J. M. van Ruitenbeek, Phys. Rev. B **48**, 14721 (1993).

[13] A. I. Yanson, Ph.D. thesis, University of Leiden, 2001.

[14] S. K. Nielsen, Y. Noat, M. Brandbyge, R. H. M. Smit, K. Hansen, L. Y. Chen, A. I. Yanson, F. Besenbacher, and J. M. van Ruitenbeek, Phys. Rev. B **67**, 245411 (2003).

[15] R. H. M. Smit, Y. Noat, C. Untiedt, N. D. Lang, M. C. van Hemert, and J. M. van Ruitenbeek, Nature (London) **419**, 906 (2002).

[16] C. Untiedt, D. M. T. Dekker, D. Djukic, and J. M. van Ruitenbeek, Phys. Rev. B **69**, 081401(R) (2004).

[17] Y. Garcia, J. J. Palacios, E. SanFabian, J. A. Verges, A. J. Perez-Jimenez, and E. Louis, Phys. Rev. B **69**, 041402(R) (2004).

[18] M. Strange, K. S. Thygesen, and K. W. Jacobsen, Phys. Rev. B **73**, 125424 (2006).

[19] V. M. Garcia-Suarez, A. R. Rocha, S. W. Bailey, C. J. Lambert, S. Sanvito, and J. Ferrer, Phys. Rev. Lett. **95**, 256804 (2005).

[20] L. de la Vega, A. Martin-Rodero, A. L. Yeyati, and A. Saul, Phys. Rev. B **70**, 113107 (2004).

[21] J. Fernandez-Rossier, D. Jacob, C. Untiedt, and J. J. Palacios, Phys. Rev. B **72**, 224418 (2005).

[22] F. Pauly, M. Dreher, J. K. Viljas, M. Häfner, J. C. Cuevas, and P. Nielaba, Phys. Rev. B **74**, 235106 (2006).

[23] A. Delin and E. Tosatti, Phys. Rev. B **68**, 144434 (2003); A. Delin and E. Tosatti, Surf. Sci. **566-568**, 262 (2004).

[24] A. Smogunov, A. Dal Corso, and E. Tosatti, Nat. Nanotechnol. **3**, 22 (2008).

[25] H. J. Choi and J. Ihm, Phys. Rev. B **59**, 2267 (1999).

[26] A. Dal Corso, A. Smogunov, and E. Tosatti, Phys. Rev. B **74**, 045429 (2006).

[27] A. Dal Corso and A. Mosca Conte, Phys. Rev. B **71**, 115106 (2005).

[28] P. Giannozzi *et al.*, http://www.quantum-espresso.org

[29] J. P. Perdew and A. Zunger, Phys. Rev. B **23**, 5048 (1981).

[30] We also explored the possibility to use the generalized gradient approximation (GGA) for *xc* functionals and eventually chose the local-density approximation (LDA) since it appears to work better for bulk Pt. In particular, it reproduces much better the experimental equilibrium lattice constant, $a=3.92$ Å. We also confronted LDA against GGA in the case of the infinite monatomic Pt chain and found that the main difference is the slightly longer equilibrium bondlength for GGA (2.40 Å) compared to LDA (2.35 Å). At the nanowire interatomic distance of 2.66 Å used in the paper, both functionals give very close values for atomic magnetic moment—0.81 μ_B (LDA) and 0.85 μ_B (GGA). Thus, we do not expect that the choice of *xc* functional actually influences our main predictions and conclusions. If anything, we should note anyway that using LDA represents a slight underestimate of magnetic tendencies. Therefore, our predicted Pt nanomagnetism is on the safe side in that respect.

[31] M. Methfessel and A. T. Paxton, Phys. Rev. B **40**, 3616 (1989).

[32] G. Rubio, N. Agrait, and S. Vieira, Phys. Rev. Lett. **76**, 2302 (1996).

[33] E. Tosatti, S. Prestipino, S. Kostlmeier, A. Dal Corso, and F. Di Tolla, Science **291**, 288 (2001).

[34] Y. Mokrousov, G. Bihlmayer, S. Heinze, and S. Blugel, Phys. Rev. Lett. **96**, 147201 (2006).

[35] M. Viret, M. Gabureac, F. Ott, C. Fermon, C. Barreteau, G. Autes, and R. Guirado-Lopez, Eur. Phys. J. B **51**, 1 (2006).

[36] G. Autes, C. Barreteau, M. C. Desjonqueres, D. Spanjaard, and M. Viret, Europhys. Lett. **83**, 17010 (2008).

[37] L. Shen, D. S. Schreiber, and A. Jarko, Phys. Rev. **179**, 512 (1969).

[38] A. Smogunov, A. Dal Corso, and E. Tosatti, Phys. Rev. B **70**, 045417 (2004).

[39] S. Hershfield, J. H. Davies, and J. W. Wilkins, Phys. Rev. Lett. **67**, 3720 (1991); Y. Meir, N. S. Wingreen, and P. A. Lee, *ibid.* **70**, 2601 (1993).

[40] E. M. Chudnovsky and L. Gunther, Phys. Rev. Lett. **60**, 661 (1988).